

BACK ANALYSES OF SOIL RETAINING WALLS FOR RAILWAY EMBANKMENTS DAMAGED BY THE 1995 HYOGOKEN-NAMBU EARTHQUAKE*

JUNICHI KOSEKI
Associate Professor
Institute of Industrial Science
University of Tokyo, Japan

MASARU TATEYAMA
Chief Engineer
Railway Technical Research Institute, Japan

FUMIO TATSUOKA
Professor, Department of Civil Engineering
University of Tokyo, Japan

KATSUMI HORII
Formerly**, Director
System Development Div.
Engineering Headquarters
Chuo Kaihatsu Corporation, Japan

ABSTRACT

In order to improve current aseismic design procedures of retaining walls, external and internal seismic stability of different types of retaining walls for railway embankment, which were damaged by the Hyogoken-nambu earthquake, was evaluated. The analysis was performed in the framework of the current design procedure based on the pseudo-static limit equilibrium method while considering the effect of vertical earthquake motion. The potential failure mode was compared with the actual behaviour, and the critical horizontal seismic coefficient which yielded a safety factor of unity was compared with the estimated peak horizontal acceleration.

Key Words: earthquake damage, railway, retaining wall, seismic coefficient, stability analysis, the 1995 Hyogoken-nambu earthquake

* The paper was published in 1996 as a part of the survey report "The 1995 Hyogoken-nambu Earthquake -An Investigation into the Damage to Civil Structures-" compiled by the Committee of Earthquake engineering, Japan Society of Civil Engineers. Here the format of the paper was changed and Figure 9 was revised

** Presently, Director, Engineering Department, Integrated Geotechnology Institute Ltd., Japan

1. INTRODUCTION

The Hyogoken-nambu Earthquake of January 17, 1995, caused serious damage to a number of conventional masonry and unreinforced concrete gravity-type retaining walls (RWs) for railway embankment. Many modern cantilever-type steel-reinforced concrete (RC) RWs were also damaged, while geogrid-reinforced soil retaining walls (GRS-RWs) having a full-height RC facing performed very well during the earthquake (Tatsuoka et al., 1996).

This paper will describe the results of back analyses by the pseudo-static limit equilibrium method on different types of the following five RWs at four sites. These analyses were conducted to evaluate the relevance of the current aseismic design procedures. The design procedures will be revised based on such analyses. Figure 1 indicates the locations of the sites and the areas where the JMA (Japanese Meteorological Agency) seismic intensity scale was seven.

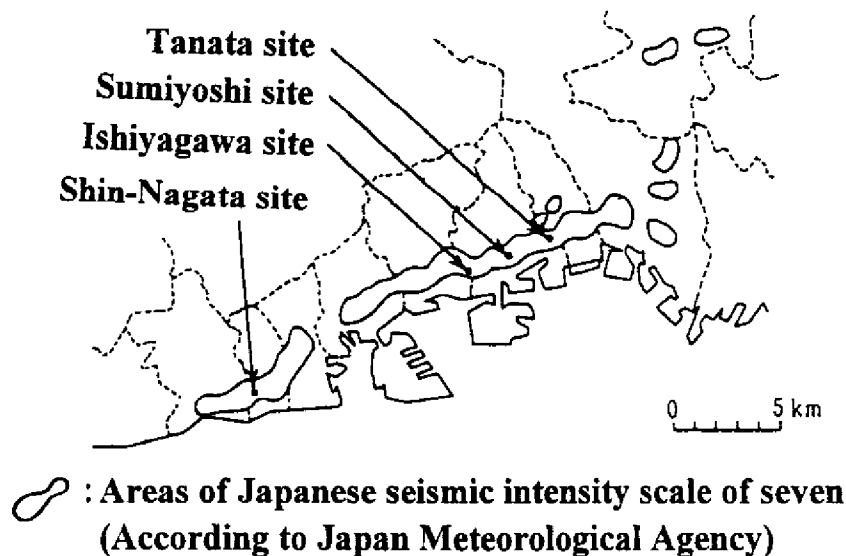


Figure 1. Areas of Japanese seismic intensity scale of seven and locations of retaining walls (RWs) reported in this paper

- a) Sumiyoshi site (Leaning-type RWs along JR Kobe Line between Setsu-Motoyama and Sumiyoshi Stations, Figure 2).

Leaning-type unreinforced concrete RWs extending for a length of about 500 m, which were constructed 58 years ago (at the time of the earthquake), were broken and split off at the level of the ground surface, and the upper part overturned completely to the ground surface, resulting into the back face upside down. In some sections where the embedment depth was relatively small, the whole RWs overturned about the bottom.

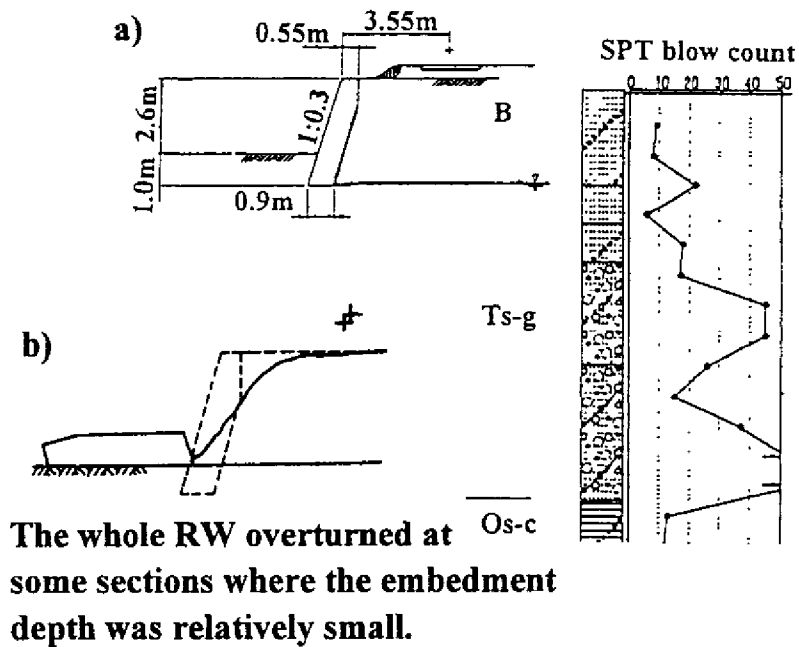


Figure 2. Leaning-type RW at Sumiyoshi site;
a) cross-section and b) sketch

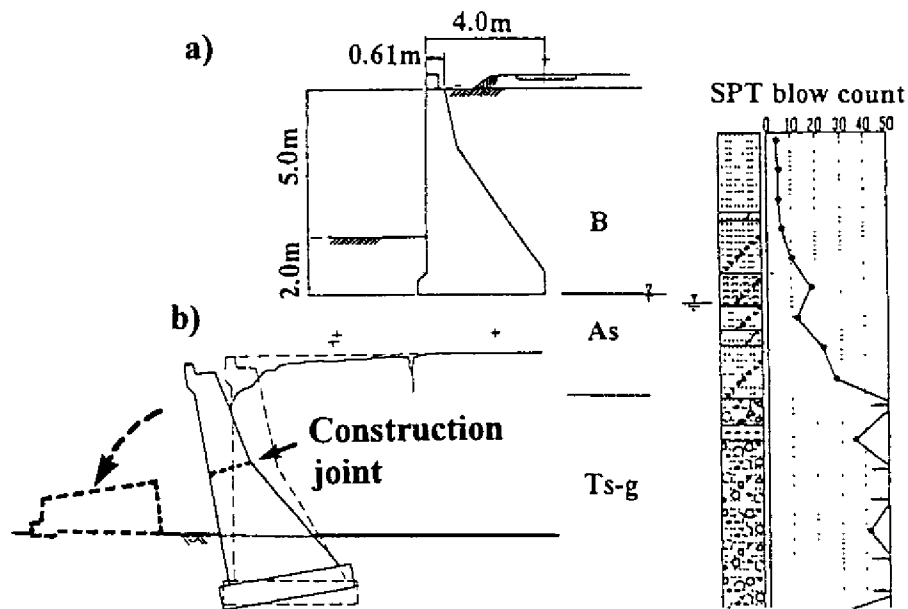
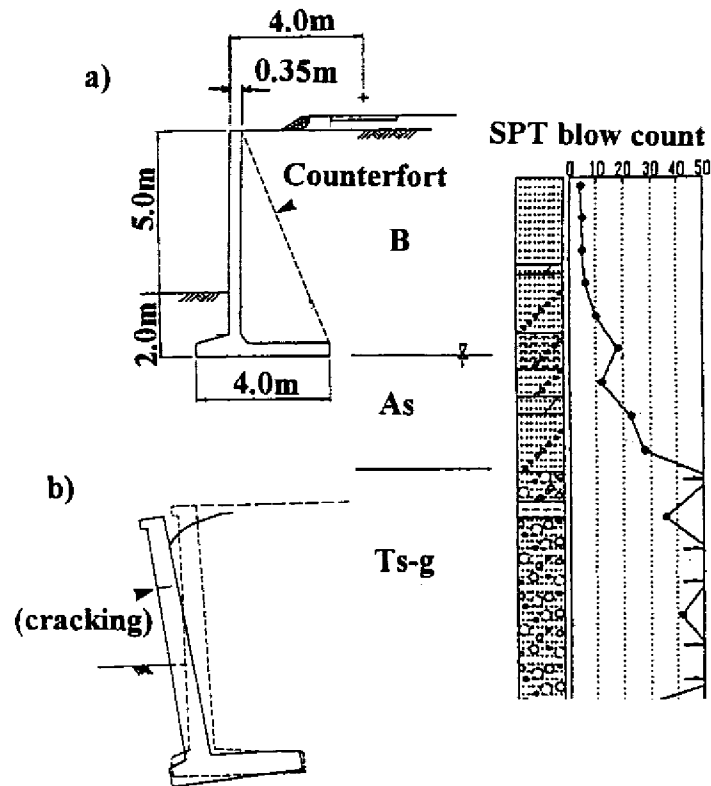


Figure 3. Gravity-type RW at Ishiyagawa site,
a) cross-section and b) sketch



**Cracking of the RC wall was observed
at a section without counterforts.**

*Figure 4. Cantilever-type RC RW at Ishiyagawa site;
a) cross-section and b) sketch*

- b) Ishiyagawa site (Gravity-type RWs, Figure 3, and cantilever-type RC RWs, Figure 4, along Main Line of Hanshin Railway Co. adjacent to Ishiyagawa Station).

Several sections of gravity-type unreinforced concrete RWs extending for a total length of about 400 m, which were constructed 66 years ago based on the standard design used at that time, tilted largely, while a 200 m-long section was broken at the construction joint at the mid-height level and overturned totally.

Cantilever-type RC RWs extending for a length of about 30 m tilted similarly to the adjoining gravity-type RW, while a section without counterforts suffered cracking at the mid-height level of the wall.

- c) Shin-Nagata site (Cantilever-type RC RWs along JR Sanyo Line at Shin-Nagata Station, Figure 5).

Cantilever-type RC RWs extending for a length of about 200 m, which were constructed 65 years ago possibly with a wooden pile foundation at the base of the RWs, suffered extensive cracking at the mid-height level of the wall and the whole RWs largely tilted and slid outward at the bottom.

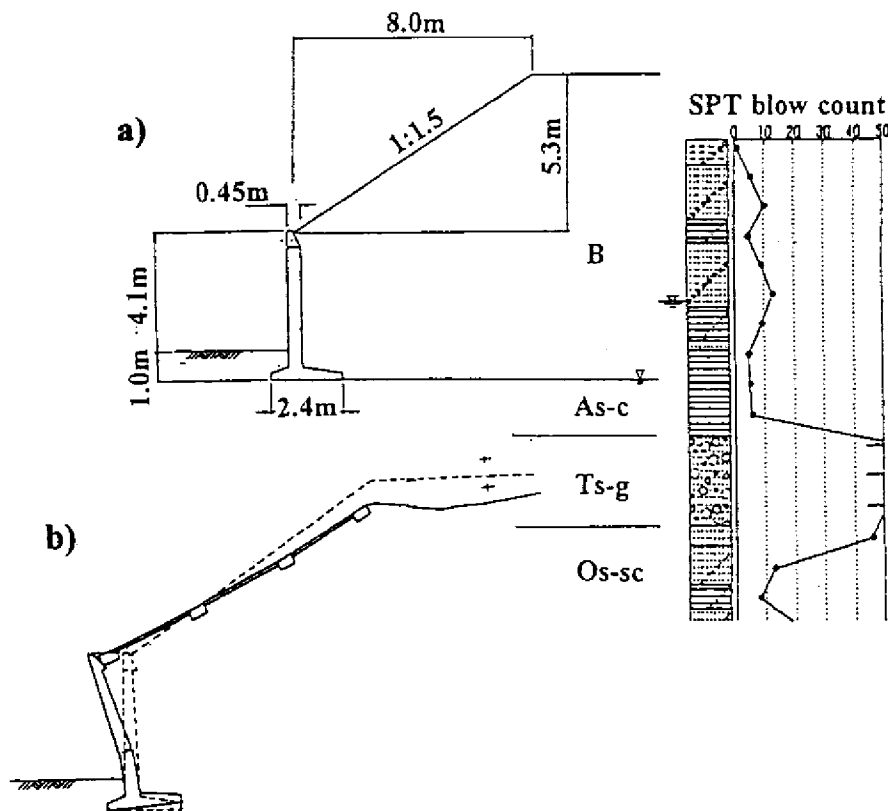


Figure 5. Cantilever-type RC RW at Shin-Nagata site;
a) cross-section and b) sketch

- d) Tanata site (GRS-RWs along JR Tokaido Line between Ashiya and Settsu-Motoyama Stations, Figure 6).

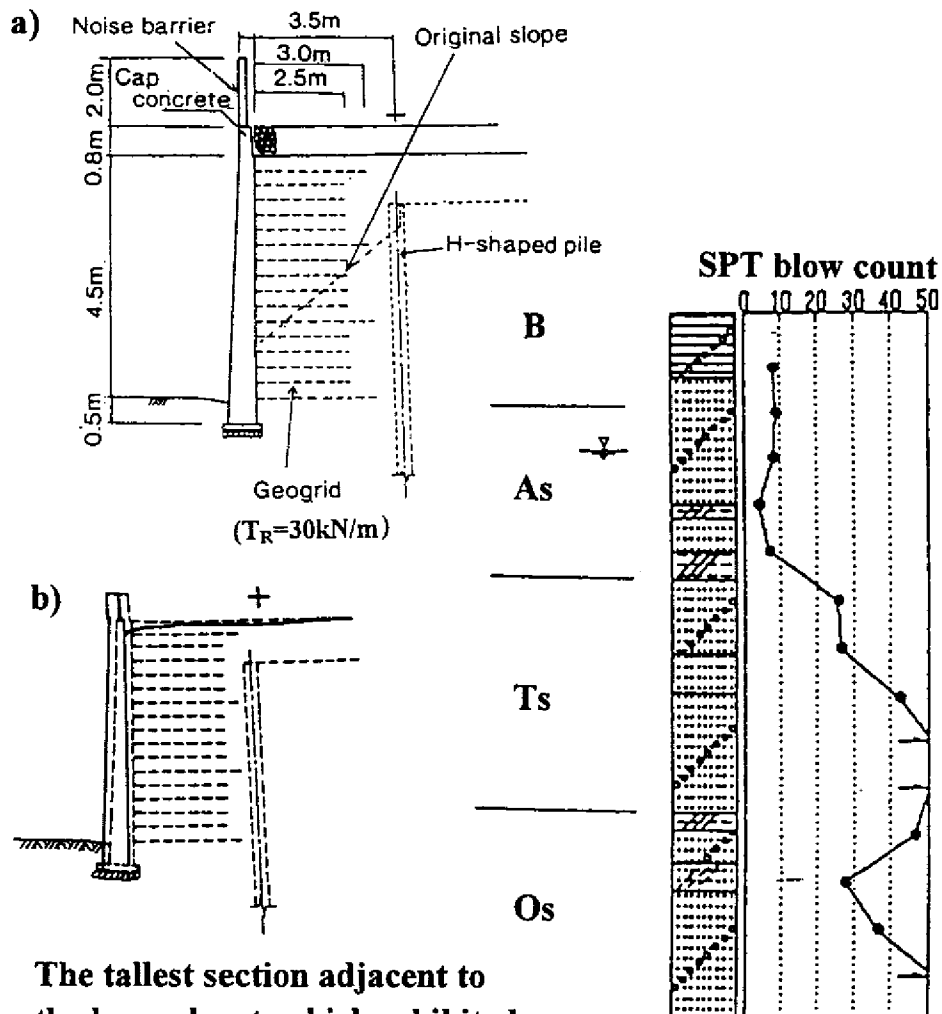
GRS-RWs having a full-height RC facing extending for a length of about 300 m, which were completed in February 1992, deformed and moved slightly. The largest outward displacement was 26 cm and 10 cm at the top of the wall and at the ground surface level, respectively, at the highest part of the wall, adjacent to a RC box culvert crossing the railway embankment.

2. SURVEY OF SUBSOIL AND EMBANKMENT CONDITIONS

Results of borehole surveys on the subsoil conditions at the typical damaged cross-section of the RWs are shown in Figures 2 to 6. The subsoils consist of, from the top, Holocene fan deposits (denoted as As and Ac in the figures), Later Pleistocene terrace deposits (Ts and Tg) and Middle Pleistocene terrace deposits (Os and Oc).

Figure 7 shows the typical grain size distributions of the fill materials for embankment. Table 1 summarizes their properties evaluated by in-situ unit weight tests. The fill material at Shin-Nagata site was a relatively loose sandy soil containing a large amount of fines, while those at other sites were Masa-soils (decomposed granite soil), which were almost similar to each

other. A series of CD triaxial compression tests on samples recompacted to the field density and water content. The confining pressures employed were relatively low, typically 9.8, 29.4, and 98 kPa , so as to simulate the field low pressure levels. The shear resistance angle ϕ_u was evaluated by assuming that the cohesion c_u be zero.



The tallest section adjacent to the box culvert, which exhibited the largest displacement, is shown.

Figure 6. GRS-RW at Tanata site;
a) cross-section and b) sketch

TABLE I

Site	In-situ unit weight test				Triaxial tests (CD) of recompacted samples			
	G_s	γ , kN/m^3	w , %	e	γ_s , kN/m^3	γ_d , kN/m^3	e	ϕ_u^* , degree
Sumiyoshi	2.630	18.04	6.7	0.525	18.04	16.91	0.525	45.8
Ishiyagawa	2.639	17.40	8.5	0.613	18.03	16.62	0.556	43.7
Shin-Nagata	2.662	16.09	10.4	0.790	15.91	14.41	0.811	35.3
Tanata	2.682	16.69	5.0	0.654	17.05	16.24	0.619	42.4

*Shear resistance angle was obtained by assuming that the cohesion c_u is zero.

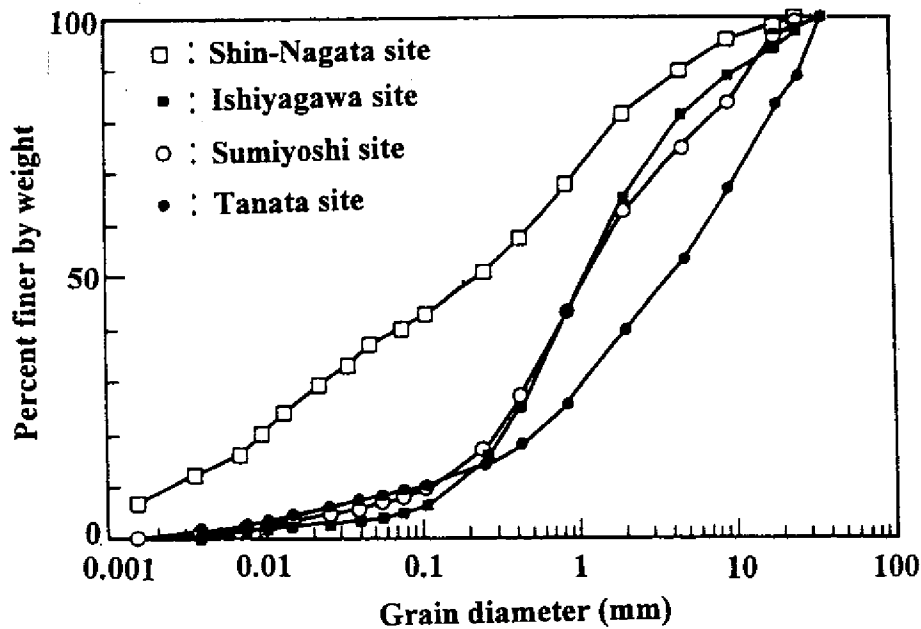


Figure 7. Grain size distribution of the fill materials for embankment

3. ESTIMATION OF PEAK GROUND ACCELERATION

Damage to wooden houses in the adjacent area of the four sites was investigated after the earthquake as summarized in Figure 8. The collapse ratios of wooden houses at and near the sites were equal to or higher than 30%. These values are consistent with the fact that all the sites were located in the most severely shaken area as shown in Figure 1. In the following analyses, the peak horizontal acceleration a_{hmax} at the four sites was roughly estimated to be between 600 and 800 cm/sec^2 , which is based on the distribution of peak ground acceleration estimated by Sato (1996) as shown in Figure 9.

4. STABILITY ANALYSES BASED ON CURRENT DESIGN PROCEDURE

In the framework of the current design procedure as specified in Design Standard for Railway Retaining Wall Structures (Japan National Railway, 1986) and Design Standard for Railway Earth Structures (Railway Technical Research Institute, 1992), stability analyses by the pseudo-static limit equilibrium method were performed to evaluate the critical seismic coefficient yielding a safety factor of unity. In the analyses, the combined effects of horizontal and vertical earthquake motion were taken into account. Analyses which consider only horizontal earthquake motion were also performed.

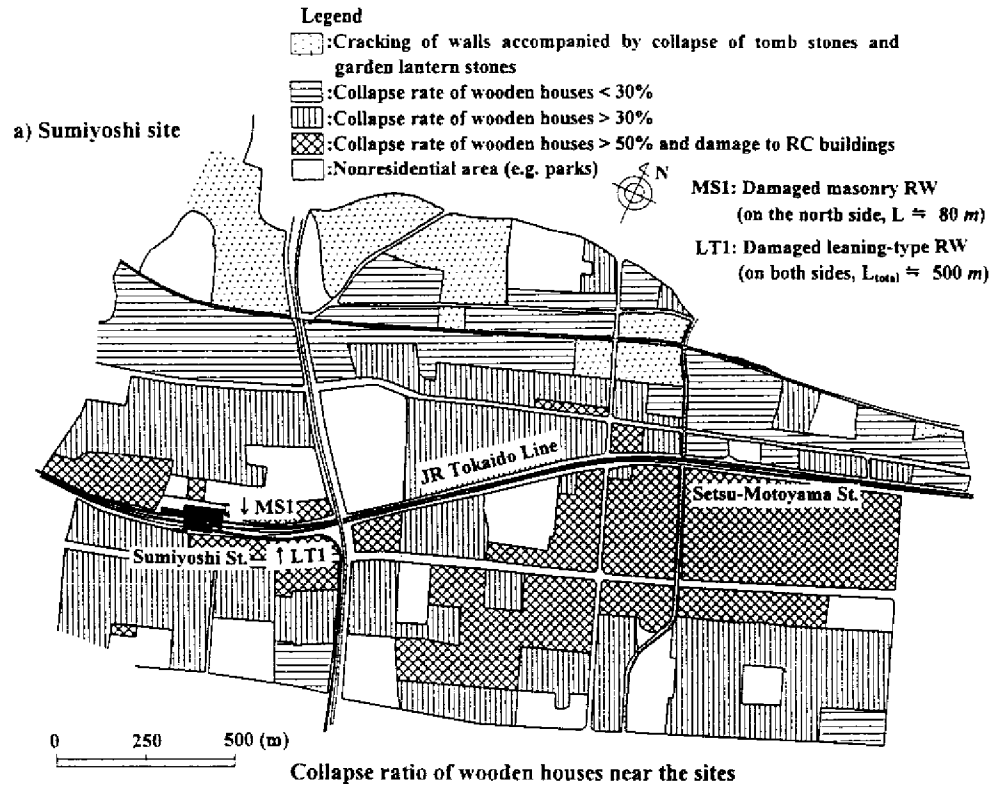


Figure 8. a) Sumiyoshi site

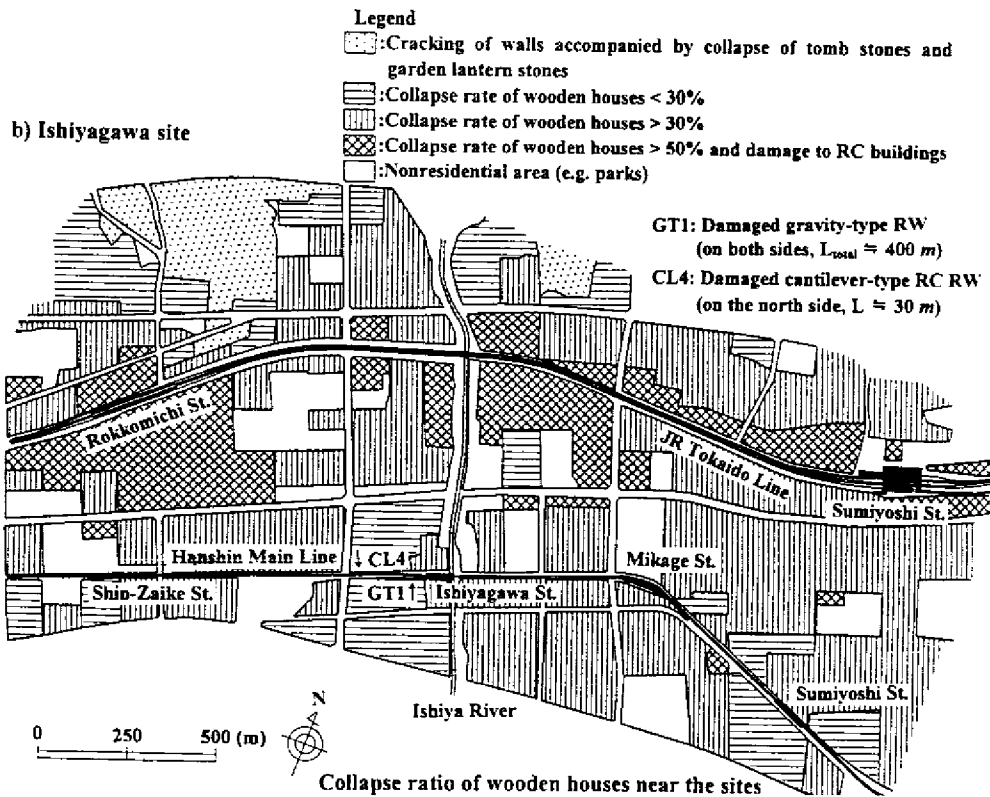


Figure 8. b) Ishiyagawa site

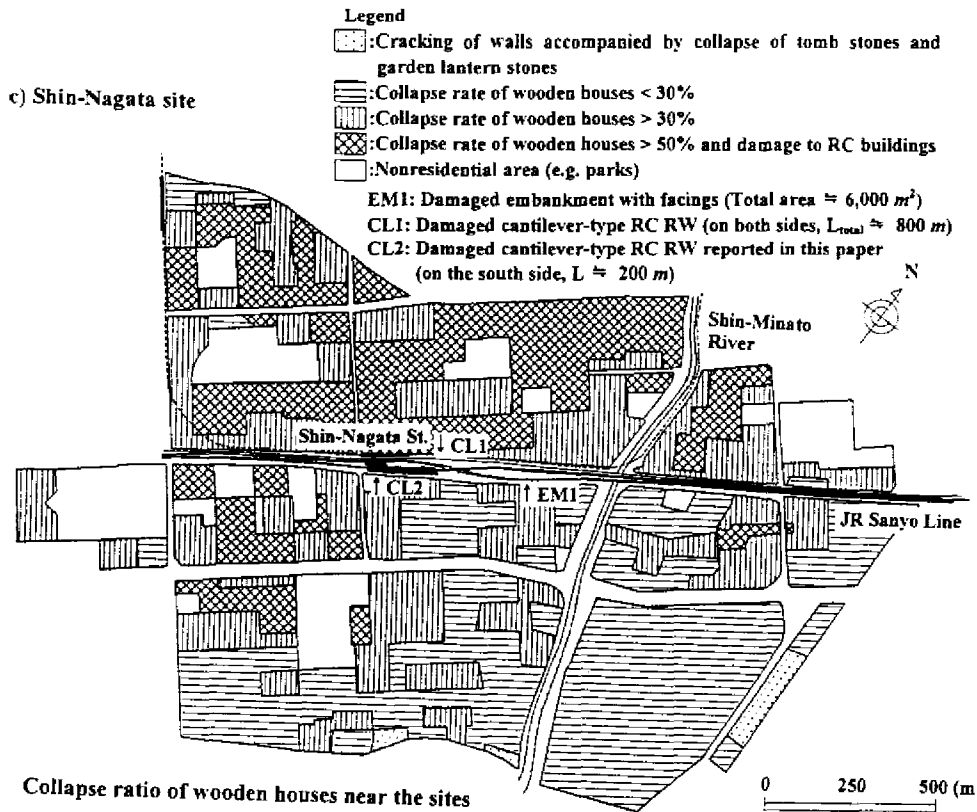


Figure 8. c) Shin-Nagata site

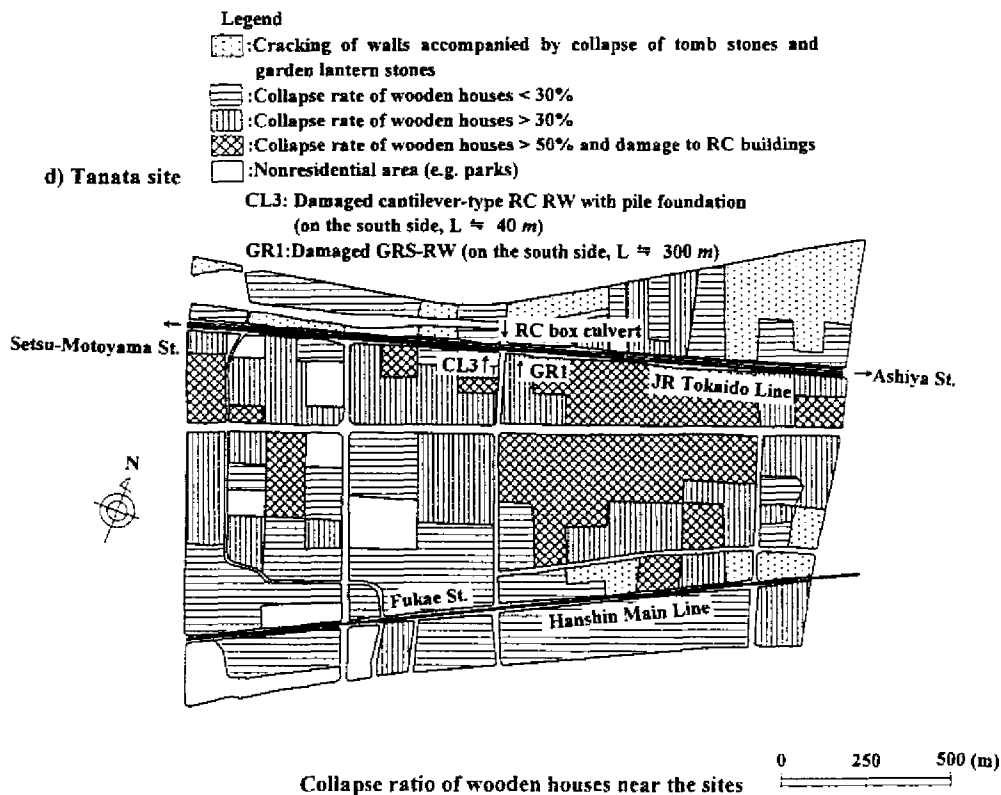


Figure 8. d) Tanata site

Figure 8. Collapse ratio of wooden houses near the sites

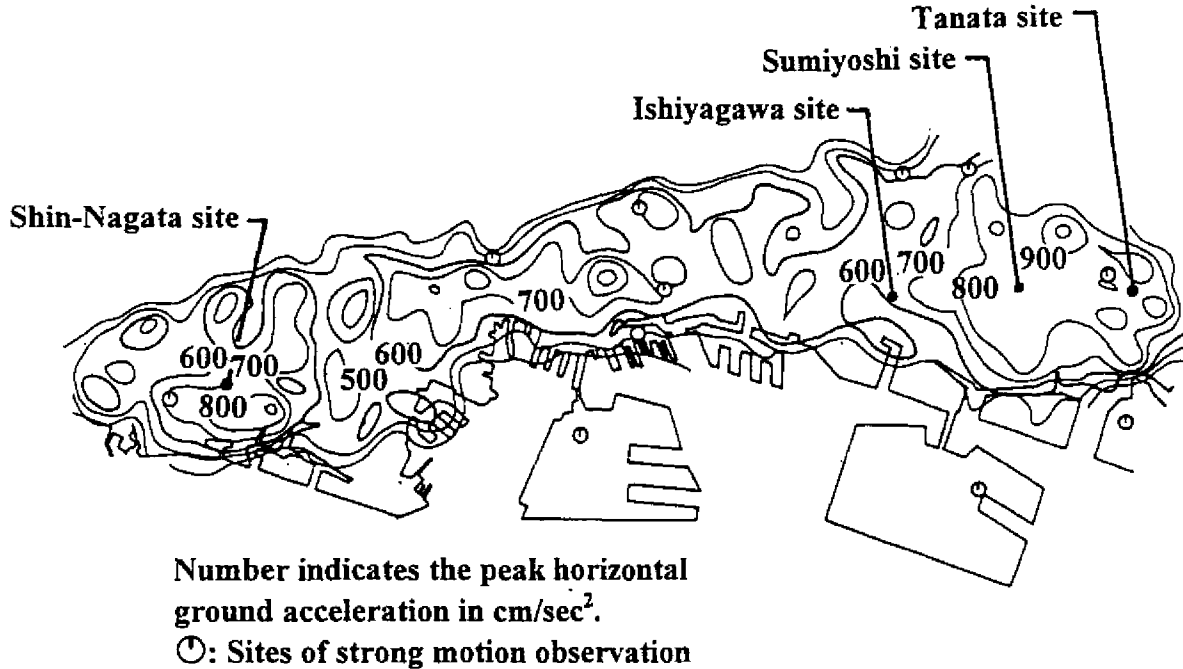


Figure 9. Estimated distribution of peak horizontal acceleration (after Sato, 1996)

(1) Design parameters

Analyses of external stability against sliding at the wall base, overturning, and bearing capacity and those of internal stability with respect to tensile and compressive failure of the concrete wall structures were conducted based on the design parameters summarized in Tables 2 and 3, respectively. The conditions of the embankment and the subsoil were determined based on the results of the in-situ and laboratory tests, while that of the concrete walls was determined from the tests on cored samples.

In the analysis of overturning stability, the center of rotation was assumed to be at the toe of the wall structure. The bearing capacity q_u of the subsoil was estimated by the following equations;

$$q_u = \{I_c \cdot \alpha \cdot c \cdot N_c + I_r \cdot \beta \cdot \gamma_1 \cdot B' \cdot N_r + I_q \cdot \gamma_2 \cdot D_f \cdot (N_q - 1)\} / F_s + \gamma_2 \cdot D_f \quad (1)$$

$$B' = B - 2 \cdot e \quad (2)$$

$$I_r = (1 - \delta_c / \phi)^2 \quad (3)$$

$$I_c = I_q = (1 - \delta_c / 90)^2 \quad (4)$$

where N_c , N_r and N_q are the coefficients of bearing capacity shown in Table 2, which were re-evaluated based on the cohesion c and the shear resistance angle ϕ estimated by the current design procedure. γ_1 and γ_2 are submerged or wet unit weight of subsoil below and above the bottom of retaining wall, respectively. α and β are the shape factors, which were assigned as $\alpha = 1.0$

and $\beta=0.5$ considering the continuity of the wall in the longitudinal direction (i.e., plane strain condition). D_f is the depth of embedment. B is the bottom width of retaining wall, and B' is the effective bottom width. e is the eccentricity of load measured from the center of the bottom of the wall. I_c , I_l , and I_q are the factors to correct for the effects of load inclination (if $\delta_L > \phi$, then $I_l = 0$), and δ_L is the direction of the inclined load in degree defined from the upward direction. In this analysis, the q_u value was obtained by ignoring the effect of the backfill soil (as in the current design procedure). This assumption, however, should be re-considered in more refined analyses.

The relationships between the coefficients of bearing capacity N_q , N_c , and N_γ and the shear resistance angle ϕ and those between the correction factors I_c , I_l , and I_q and the direction of the inclined load δ_L according to the current design procedure are shown in Figures 10 and 11, respectively.

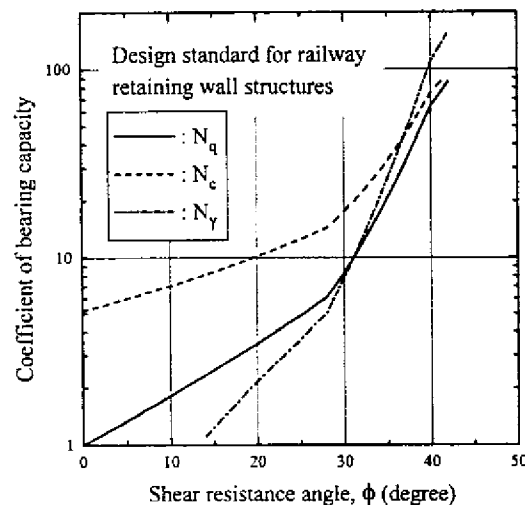


Figure 10. Relationships between coefficients of bearing capacity and shear resistance angle

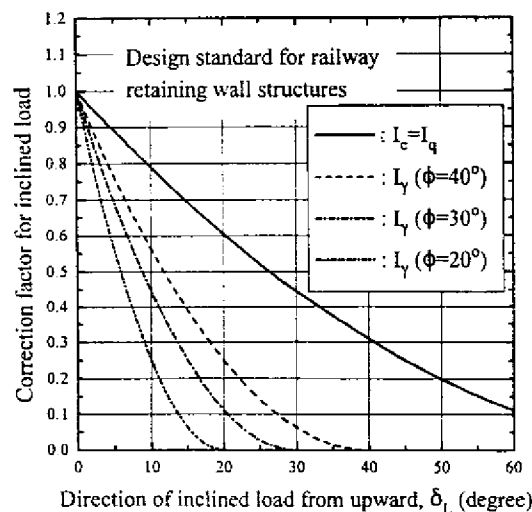
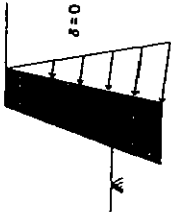
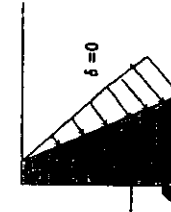
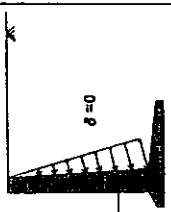
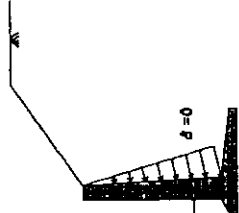
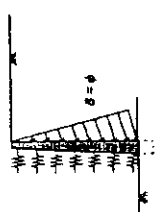


Figure 11. Relationships between correction factors and direction of inclined load

TABLE 3. DESIGN PARAMETERS FOR INTERNAL STABILITY ANALYSES

Site	Sumiyoshi (Leaning type)	Ishiyagawa (Gravity type)	Ishiyagawa (Cantilever type)	Shin-Nagata (Cantilever type)	Tanata (GRS-RW)
Schematic diagram					
Concrete γ	23.2	22.7	22.5	23.2	24.5
Compressive strength (kN/m ²)	18.6	18.8	30.5	25.8	20.6
Tensile strength (kN/m ²)	1.66	1.41	2.47	2.26	-
Steel bar Tensile strength (MN/m ²)	-	-	481	481	481
Cross-sectional Area (m ² /m)	-	-	77.6x10 ⁻⁴	19.4x10 ⁻⁴	5.08x10 ⁻⁴

(2) Consideration of vertical earthquake motion

To take into account the effects of vertical earthquake motion, the earth pressure acting from the backfill soil was evaluated by the trial wedge method as schematically shown in Figure 12 while considering the cross-sectional shape of the embankment and the vertical inertia force acting on the trial wedge. The location of the bottom apex of the triangle was fixed at the bottom of the actual or virtual back face of the wall structure while the angle α was changed to obtain the maximum earth pressure. The combination of the horizontal and vertical seismic coefficients was assigned as

$$k_{h,i} = R \cdot (a_{h,i} / g) \quad (5)$$

$$k_{v,i} = R \cdot (a_{v,i} / g) \quad (6)$$

$$R = k_h / (a_{h,max} / g) \quad (7)$$

where $a_{h,i}$ and $a_{v,i}$ are the i th combination of the horizontal and vertical acceleration amplitudes obtained from the strong motion records in the N-S and UP directions at Kobe Marine Meteorological Observation Station as shown in Figure 13. g is the gravitational acceleration, and $k_{h,i}$ and $k_{v,i}$ are the corresponding i th horizontal and vertical seismic coefficients. $a_{h,max}$ is the recorded peak horizontal acceleration (579 cm/sec² in the north direction and 818 cm/sec² in the south direction). R is the factor introduced to adjust each acceleration amplitude so that the maximum of $k_{h,i}$ becomes equal to the nominal horizontal seismic coefficient k_h . For external stability analyses, the value of k_h was varied between 0 and about 1.0, while for internal stability analyses it was increased beyond 1.0 until the safety factor of unity was obtained.

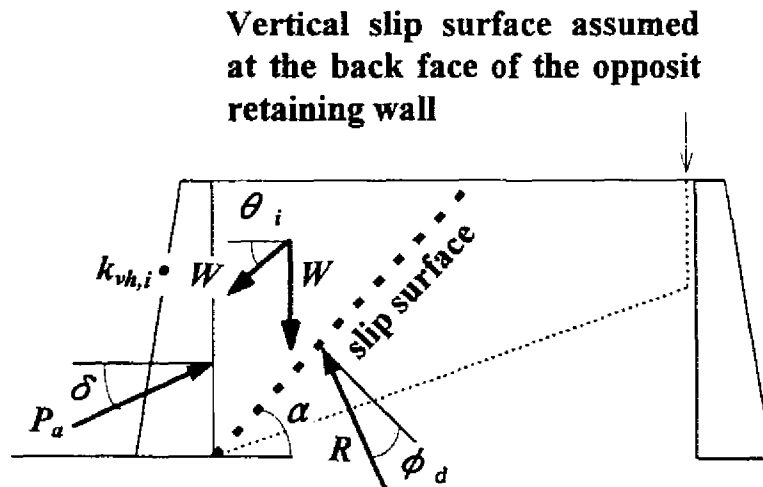


Figure 12. Schematic diagram on trial wedge method

To prepare Figure 13, resultant acceleration $a_{r,i}(t)$ and its direction $\theta(t)$ defined from the upward direction were calculated from the recorded horizontal and vertical accelerations $a_h(t)$ and $a_v(t)$ at time t .

$$a_{r,i}(t) = (a_h(t)^2 + a_v(t)^2)^{1/2} \quad (8)$$

$$\theta(t) = \tan^{-1}(a_h(t)/a_v(t)) \quad (9)$$

At intervals of 10 degrees, the lapse of $\theta(t)$ was divided into several time steps, and the combination of $a_h(t)$ and $a_v(t)$, which yields the peak amplitude of $a_{r,i}(t)$ for each time step, was plotted in Figure 13. In the stability analyses, combinations of these accelerations corresponding to the outer envelope of the distribution were employed.

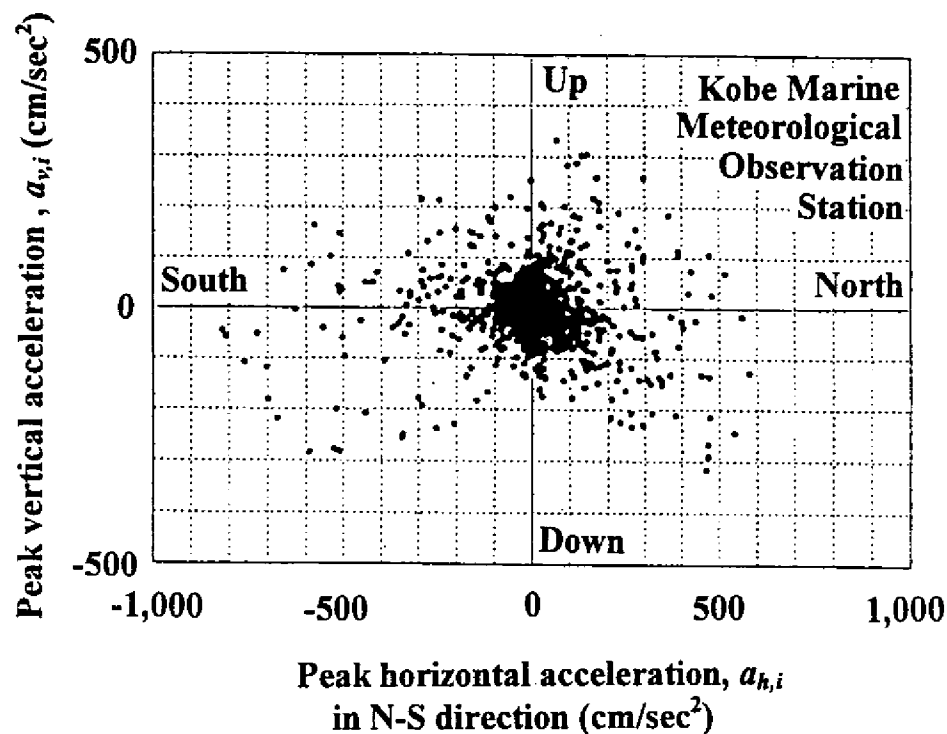


Figure 13. Horizontal and vertical acceleration amplitudes obtained from the strong motion records in the N-S and U-D direction at Kobe Marine Meteorological Observation Station

The retaining wall at Sumiyoshi site and the cantilever-type one at Ishiyagawa site were located on the north of the respective embankment, while the gravity-type one at Ishiyagawa site and the other type walls at Shin-Nagata site and Tanata site were located on the south of the respective embankment. In the stability analyses, the following three cases were examined expediently with respect to this directionality. In case N, positive northbound acceleration was converted to positive horizontal seismic coefficient corresponding to an outward inertial force. Similarly, positive southbound acceleration was employed as outward inertial force in case S. In these cases, downward acceleration was taken as positive to yield the positive vertical seismic coefficient corresponding to upward inertial force.

On the contrary, the effects of vertical earthquake motion was not considered in case H.

In case N and case S, a series of resultant seismic coefficients $k_{th,i}$ and their direction θ_i defined from the upward direction (refer to Figure 12) were obtained from the i th combination of the horizontal and the vertical seismic coefficients, $k_{h,i}$ and $k_{v,i}$, as follows.

$$k_{th,i} = (k_{h,i}^2 + k_{v,i}^2)^{1/2} \quad (10)$$

$$\theta(i) = \tan^{-1}(k_{h,i}/k_{v,i}) \quad (11)$$

These values were used to find the active earth pressure by changing the angle α of the slope of the potential failure surface. In so doing, the active earth pressure was assumed to distribute vertically similar to hydrostatic pressure. By this way, the safety factor for each of the aforementioned failure modes for a given nominal horizontal seismic coefficient k_h was defined as the minimum value of those for all the combinations of $k_{th,i}$ and θ_i . By repeating this procedure, the relationship between the safety factor and the nominal horizontal seismic coefficient k_h was obtained for each failure mode.

Note that the effects of earthquake motion on the subsoil below the ground surface was not considered in evaluating the active and the passive earth pressure, while the inertial force F for the wall structure embedded below the ground surface was reduced by the following equation;

$$F = k_h \cdot (W - \gamma_2 \cdot V) \quad (12)$$

where W and V are weight and volume of the wall structure embedded below the ground surface, respectively, and γ_2 is the wet unit weight of subsoil above the bottom of retaining wall.

(3) Safety factors for external stability

Safety factors for external stability of each case for the leaning-type RW at Sumiyoshi site are compared in Figure 14. Within the range of the assumed combination of horizontal and vertical acceleration amplitudes (Figure 13), the effect of vertical earthquake motion on the safety factors at the same nominal horizontal seismic coefficient k_h was very small. This tendency was also observed in the other results of stability analyses at all sites.

For each RW, relationships between the nominal horizontal seismic coefficient k_h and the safety factor for external stability for case N are shown in Figure 15. The potential failure mode which yields the smallest seismic coefficient is that due to the lack of bearing capacity in the subsoil layer beneath the wall for the gravity-type RW at Ishiyagawa and the cantilever-type RC-RWs at Ishiyagawa and Shin-Nagata, while it is overturning and sliding for the leaning-type RW at Sumiyoshi and the GRS-RW at Tanata,

respectively. Note that the safety factor against bearing capacity is taken as zero when overturning failure is expected to occur. Therefore, for Sumiyoshi site, the zero safety factor for bearing capacity failure shown in Figure 15(a) is only the result of the safety factor becoming less than unity for overturning, and it has no indication for the potential bearing capacity failure.

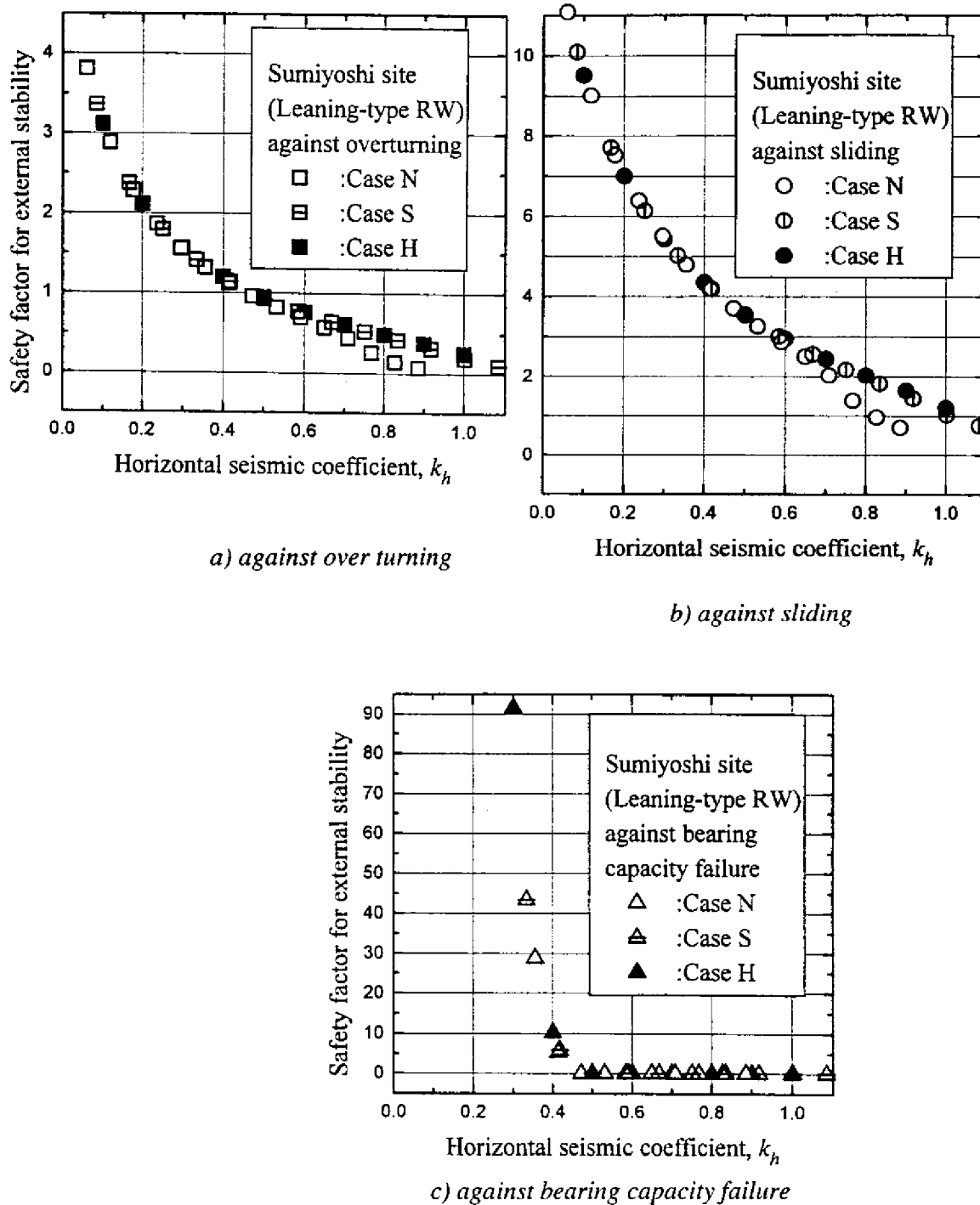


Figure 14. Effects of vertical earthquake motion on the safety factor for external stability of the leaning-type RW at Sumiyoshi site

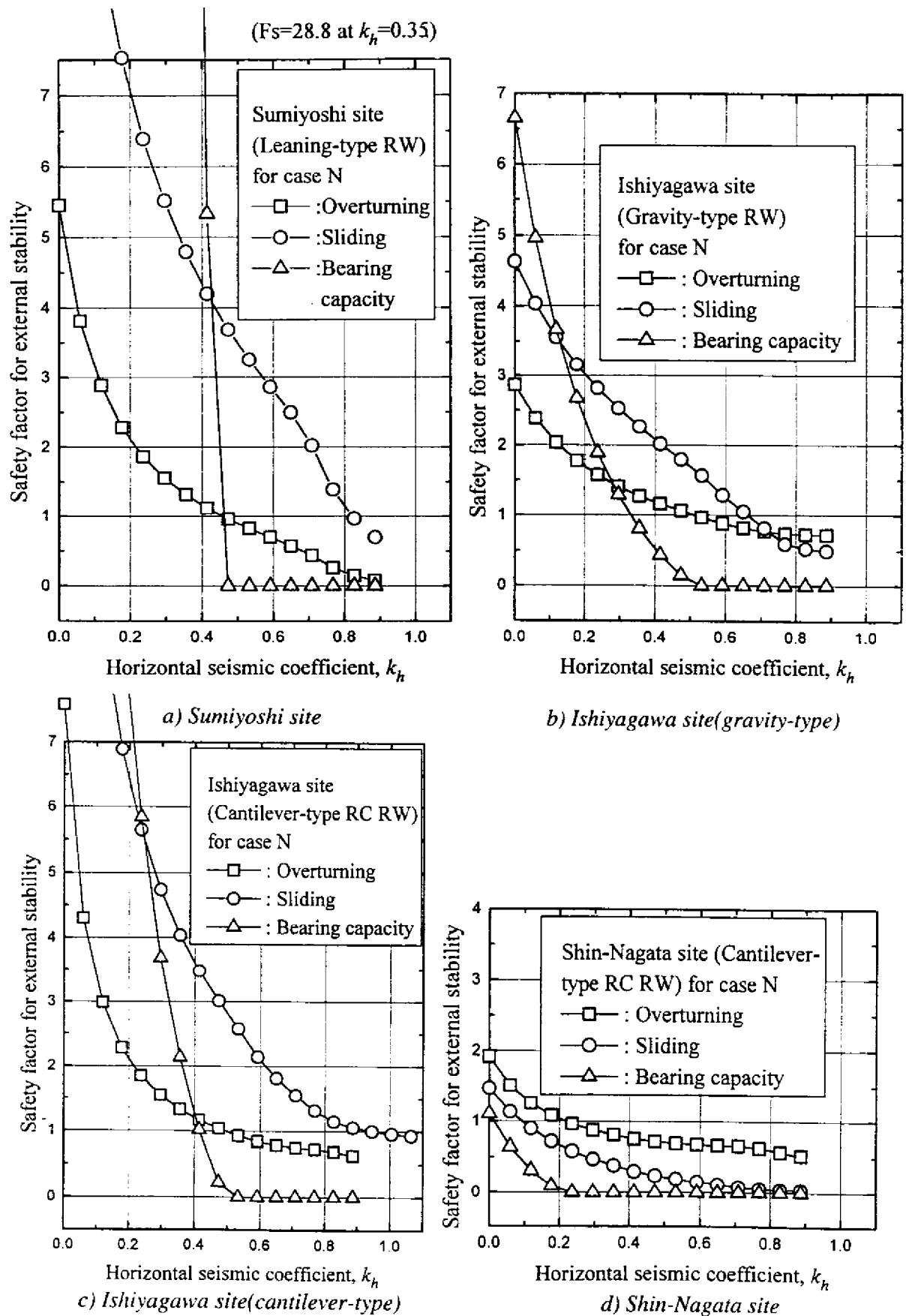
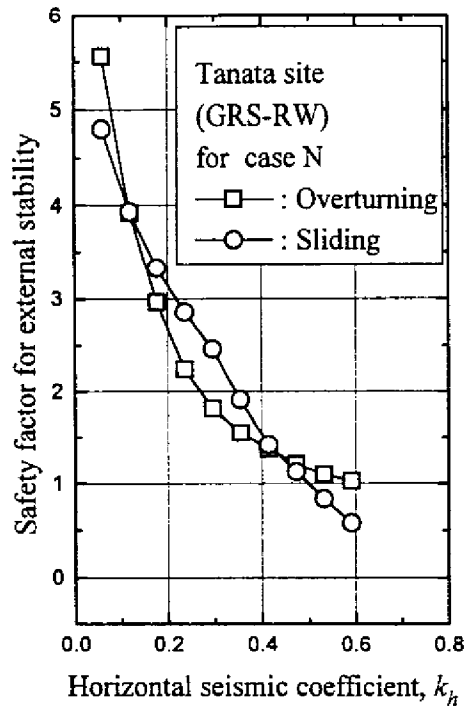


Figure 15 (to be continued)



e) Tanata site

Figure 15. Relationships between the horizontal seismic coefficient and the safety factors for external stability

For the GRS-RW at Tanata, the bearing capacity failure at the bottom of the facing was not considered, since the wall can maintain its stability even when the load acting at the bottom of the facing reaches the bearing capacity of the subsoil, as demonstrated by a large-scale shaking test on a model of GRS-RW (Murata et al., 1994). In this test, the bearing capacity of the saturated sand below the facing of the model wall with a height of 2.5 m was lost by liquefaction by shaking and the facing settled down about 1 cm relative to the reinforced backfill. Despite the above, the stability of the model wall was maintained during and after shaking. In the analysis, when the safety factor for bearing capacity was going to become less than unity, the direction of the earth pressure acting on the back face of the facing was inclined more horizontally so that the safety factor did not become less than unity. By doing so, the horizontal component of the earth pressure resisted by the reinforcement increased. In the design procedure, when the bearing capacity of the subsoil below the facing is found not sufficient, the reinforcement layers are re-arranged so as to maintain the wall stability.

For the RWs at Sumiyoshi, Ishiyagawa and Tanata sites, the expected failure modes are consistent with the observed ones as far as external instability is concerned. It is to be noted, however, that at Shin-Nagata site, the safety factor against bearing capacity failure without seismic effect (i.e. $k_h = 0$) is already less than unity. This unrealistic result may be attributed to possible existence of wooden piles used to reinforce the subsoil underlying the wall, which are indicated in the original design plans. Their contribution, however, was ignored in the stability analyses shown above. During the restoration work after the earthquake, it was attempted to identify the piles

by excavating the subsoil partly, but they were not found. In spite of this, their existence, which alters substantially the potential failure mode of the wall for external stability from bearing capacity failure to sliding, was assumed in the following analyses considering the fact that the wall had been actually stable before the earthquake.

From the above, the critical nominal horizontal seismic coefficients $k_{h,crit}$ which yield the safety factor of unity for case N were evaluated as 0.46 for the leaning-type RW at Sumiyoshi, 0.33 for the gravity-type RW at Ishiyagawa, 0.42 for the cantilever-type RC RW at Ishiyagawa, 0.09 for the cantilever-type RC RW at Shin-Nagata and 0.50 for the GRS-RW at Tanata site, respectively. These values are listed in Table 4 together with corresponding potential failure modes and the values of $k_{h,crit}$ for case S and case H.

TABLE 4. POTENTIAL FAILURE MODES AND CRITICAL SEISMIC COEFFICIENTS FOR EXTERNAL AND INTERNAL STABILITY

Site		Sumiyoshi	Ishiyagawa	Ishiyagawa	Shin-Nagata	Tanata
Type of RW		Leaning	Gravity	Cantilever	Cantilever	GRS
$k_{h,crit}$ for external stability	Failure mode	Overturning	Bearing capacity	Bearing capacity	Sliding	Sliding
	Case N	0.46	0.33	0.42	0.09*	0.50
	Case S	0.47	0.33	0.43	0.09*	0.50
	Case H	0.48	0.34	0.44	0.09*	0.50
$k_{h,crit}$ for internal stability	Failure mode	Tensile failure	Tensile failure	Tensile failure**	Tensile failure	-
	Case N	0.70	0.98	0.71	0.24	-
	Case S	0.76	1.11	0.76	0.24	-
	Case H	0.77	1.14	0.78	0.23	-

*At Shin-nagata site, potential failure mode was obtained by assuming existence of wooden piles in subsoil beneath the RW.

**For cantilever-type RC RW at Ishiyagawa site, critical seismic coefficients for internal stability were almost similar for both compressive and tensile failure.

In these external stability analyses, the possible link between the bearing capacity failure and the overturning failure was not considered. It is quite possible that the center of rotation cannot be located at the toe of the wall by the yielding in the subsoil beneath the toe of the wall. Instead, the center of rotation should be located more inside back of the wall toe, which leads to the decrease in the safety factor against overturning failure. One more realistic assumption would be such that the center of the rotation is located at the center of the effective bottom width B' for which the safety factor for bearing capacity is equal to unity. This factor is particularly important for a rigid wall structure having a relatively wide base, i.e., gravity-type and cantilever-type RC RWs. Therefore, in analyses taking into account this factor, the safety factor against overturning failure for Ishiyagawa and Shin-Nagata sites will become lower than those shown in Figure 15. This issue is beyond the scope of this paper and will be studied in the near future.

(4) Safety factors for internal stability

Figure 16 shows relationships between the nominal horizontal seismic coefficient k_h and the safety factors for internal stability of each RW for case N, where the safety factors were plotted on a logarithmic scale because they changed very largely with changes in the seismic coefficient. For all the

RWs, the safety factors against tensile failure of wall structure (reinforcing steel bar for GRS-RW and unreinforced concrete for other RWs) were smaller than those against compressive failure of wall structure, while the difference in the safety factors for the cantilever-type RC RW at Ishiyagawa site was very small. The critical horizontal seismic coefficients which yield a safety factor of unity for case N were 0.70 for the leaning-type RW at Sumiyoshi, 0.98 for the gravity-type RW at Ishiyagawa, 0.71 for the cantilever-type RC RW at Ishiyagawa, and 0.24 for the cantilever-type RC RW at Shin-Nagata site, respectively. These values are also listed in Table 4. The critical coefficient for the gravity-type RW at Ishiyagawa site should be even smaller if the reduced strength at the construction joint is taken into account in the analyses.

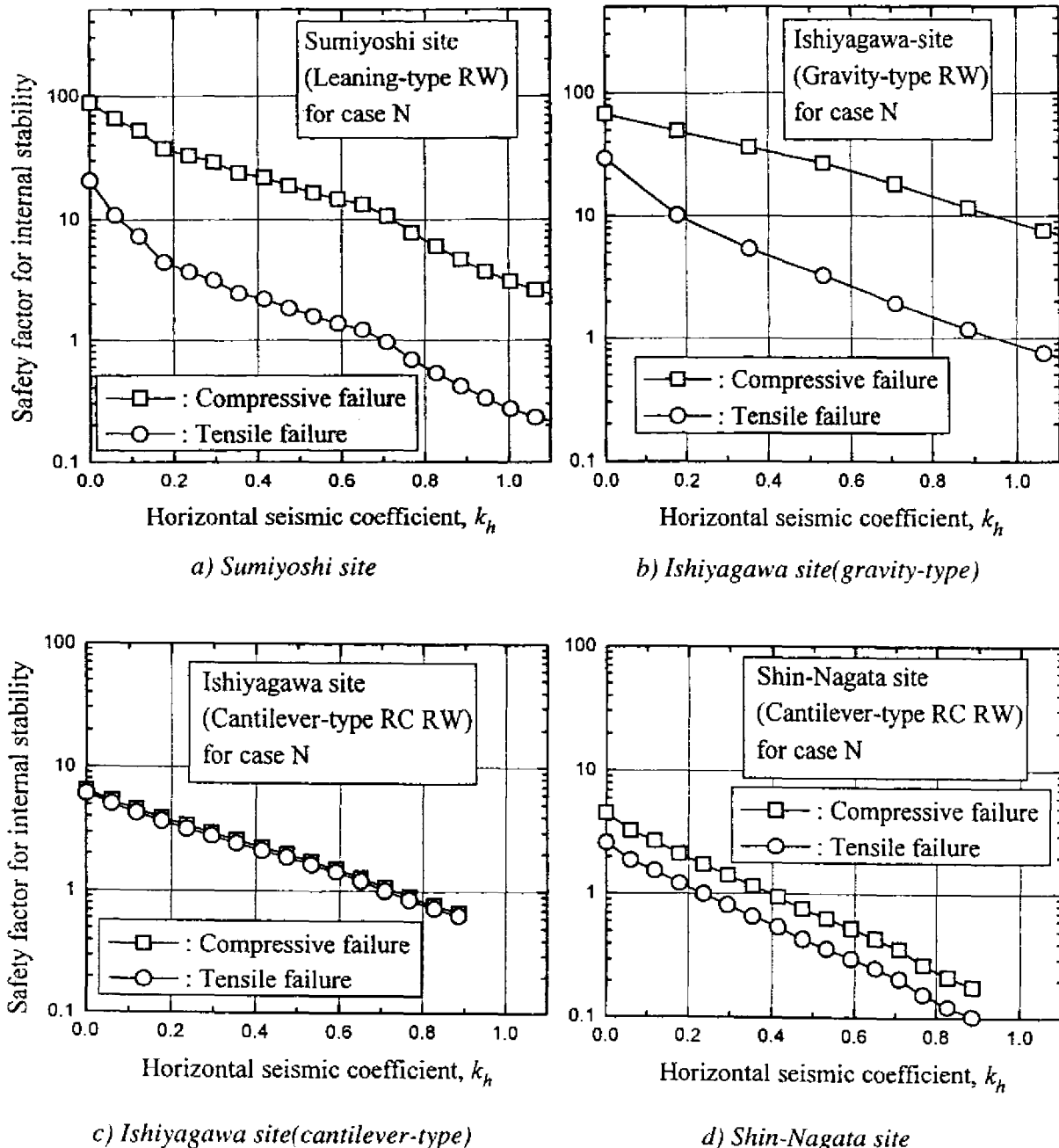
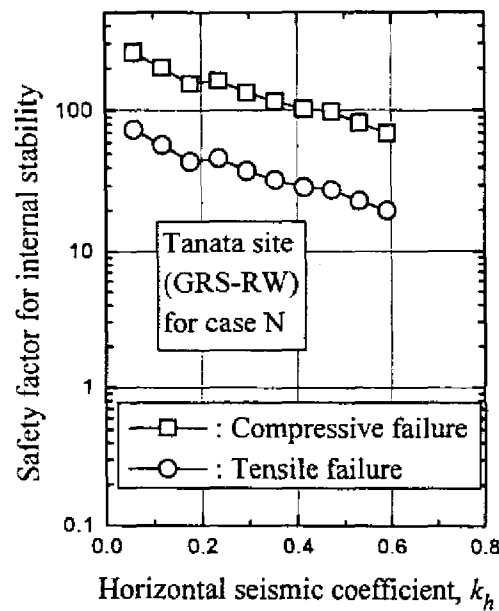


Figure 16 (to be continued)



e) Tanata site

Figure 16. Relationships between the horizontal seismic coefficient and the safety factors for internal stability

It should be noted that the safety factor for internal stability at Tanata site was always larger than 1.0, which supports the fact that the facing of the GRS-RW was not damaged. This fact demonstrates that the facing with a minimal width of 30 to 55 cm was strong enough to survive the earthquake. This high safety factor, despite a relatively small facing thickness, is due to the fact that the facing behaves like a continuous beam supported by a number of points with a short span equal to a small vertical spacing of reinforcement layers, 30 cm. This is in contrast with the fact that the other types of retaining walls behave like a cantilever beam supported only at the base.

5. CORRECTION FACTORS

Obviously, the use of the peak horizontal acceleration divided by g as the horizontal seismic coefficient in the pseudo-static limit equilibrium-based stability analysis is not appropriate, but the value corrected by being multiplied by a factor C less than unity should be used. The correction factor C can be defined as

$$C = k_{h,crit} / (a_{hmax,crit} / g) \quad (13)$$

Where $a_{hmax,crit}$ is the critical peak horizontal acceleration which just triggers failure of the wall, and $k_{h,crit}$ is the equivalent critical horizontal seismic coefficient which yields a safety factor of unity by the pseudo-static limit equilibrium-based stability analysis.

In this study, $k_{h,crit}$ for external and internal stability was evaluated for the five RWs at the four sites as mentioned in the preceding section excluding that at Tanata site for internal stability. To estimate the value C for each case, the value of $k_{h,crit}$ was divided by the ratio of the estimated range of the peak horizontal acceleration a_{hmax} which was between 600 and 800 cm/sec², to g , which yields the ratio;

$$C_r = k_{h,crit} / (a_{hmax} / g) \quad (14)$$

The C value should be larger than the value of C_r for a RW which actually failed, because a_{hmax} should be larger than $a_{hmax,crit}$. On the other hand, the value of C should be smaller than the value of C_r for a wall which did not fail but may fail for the peak ground acceleration larger than a_{hmax} .

Figure 17 shows the values of C_r for external stability obtained from the analyses for case N considering the effects of vertical acceleration. It may be seen that the values of C_r are between 0.4 and 0.8 except for the cantilever-type RC RW at Shin-Nagata site. The value of C_r as small as about 0.1 for the cantilever RC RW at Shin-Nagata site may be consistent with the actual extent of failure that the displacement of the wall during the earthquake was much larger than that of the cantilever RC RW at Ishiyagawa site.

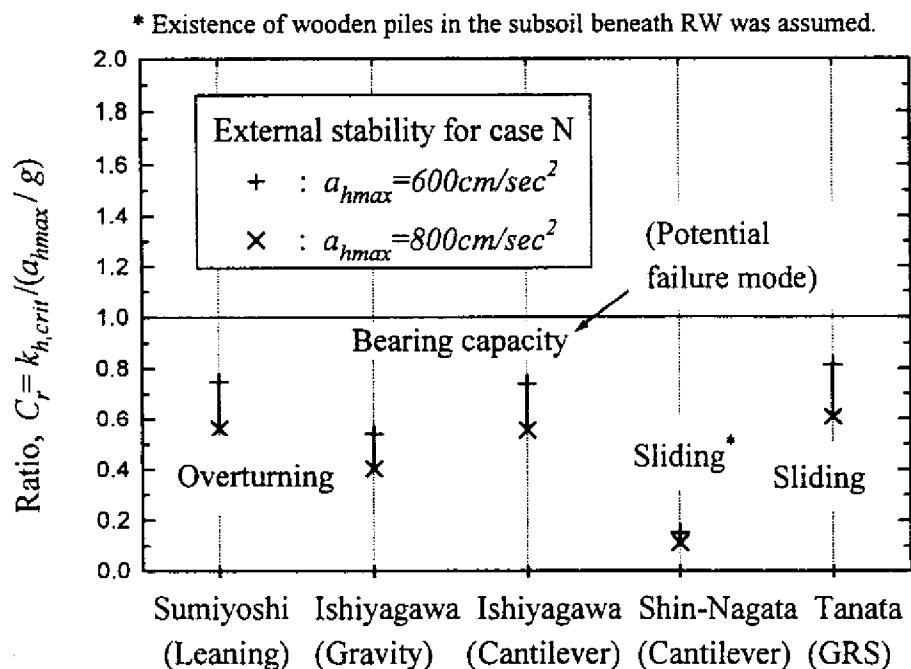


Figure 17. Ratio of critical seismic coefficient to estimated peak horizontal acceleration for external stability

In comparison with the leaning-type RW at Sumiyoshi and the gravity-type one at Ishiyagawa site, which were seriously damaged and removed for reconstruction after the earthquake, GRS-RW at Tanata site was only slightly damaged and has been reused at the slightly displaced position. However, the C_r values are similar between them. This inconsistent result may have resulted from inconsistencies in the current design methods for

these different types of RWs. Based on the actual damage and the need for reconstruction, the actual value of C to be adopted for external stability analysis in the framework of the current design standards may be larger than about 0.6 (but less than 1.0) for the leaning-type, gravity-type and cantilever-type RWs, while this value may be smaller than 0.6 for GRS-RWs. Ductile behaviour of GRS-RW together with hidden conservatism in its current design procedure was discussed by Tatsuoka et al. (1996), but it is still a matter for further study.

The values of C_r for internal stability for case N are indicated in Figure 18. For the gravity-type RW at Ishiyagawa site, the correction factor is as high as about 1.4, which should become much smaller when the strength reduction at the construction joint is taken into account. This may lead to a consistency with the fact that a section of the gravity-type wall was totally broken and split off at the construction joint at the mid-height level as mentioned before. On the other hand, a value of C_r as low as about 0.3 evaluated for the cantilever-type RW at Shin-Nagata site may reflect the fact that the wall suffered extensive cracking at the mid-height level. In contrast to these, the value is around 1.0 for the leaning-type RW at Sumiyoshi site and the cantilever-type RC RW at Ishiyagawa site. This value of C_r may be consistent with the occurrence of partial breakage and overall cracking in these RWs, respectively. This result indicates only that the correct value of C_r should be around unity. Comparison of this value with the corresponding range for external stability shown in Figure 17 leads to a suggestion that the actual value of C to be used for internal stability analysis should be larger than that for external stability analysis.

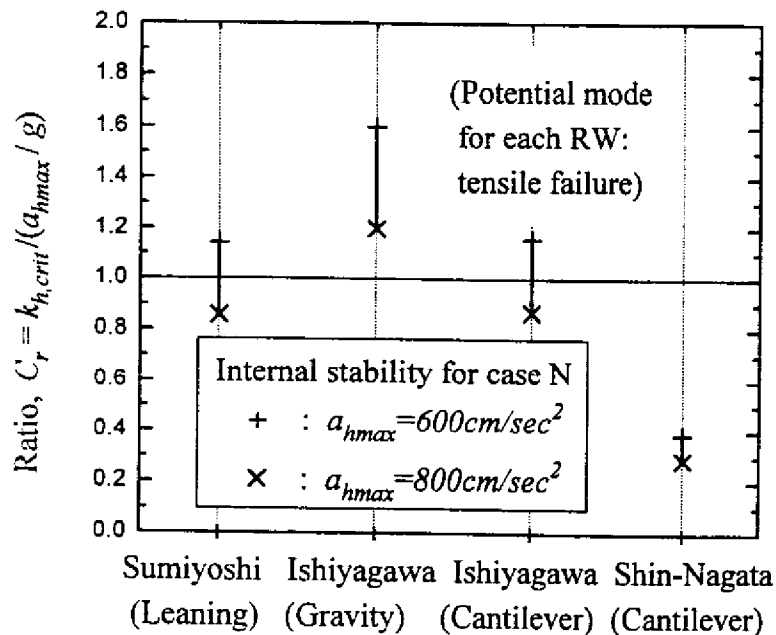


Figure 18. Ratio of critical seismic coefficient to estimated peak horizontal acceleration for internal stability

6. CONCLUSIONS

A variety of retaining walls for railway embankment in areas shaken severely by the 1995 Hyogoken-nambu earthquake performed differently. The potential failure mode expected from the results of pseudo-static limit equilibrium-based stability analyses based on the current design procedure were generally consistent with the observed behaviour. In the analysis, the effect of vertical earthquake motion on the results was found to be almost negligible.

The correction factor C was defined as the ratio of the critical horizontal seismic coefficient, which yields a safety factor of unity, to the coefficient corresponding to the ratio of the estimated peak horizontal acceleration which triggers failure to the gravitational acceleration. It was estimated that for seriously damaged walls (leaning-type, gravity-type and cantilever-type RC RWs), a value of C larger than 0.6 (but very likely less than 1.0) should be used to convert the design peak horizontal acceleration divided by g into the design seismic coefficient to be used in the pseudo-static limit equilibrium-based external stability analysis. On the contrary, it was suggested that for geogrid-reinforced soil RWs, a value of C equal to 0.6 for external stability is still conservative. Furthermore, it was suggested that the correction factor for internal stability may be larger than these values for external stability.

Further investigation is required on the difference in this factor for different types of RWs including that on the effects of the ductile behaviour of GRS-RW together with the hidden conservatism in its design procedure.

ACKNOWLEDGMENTS

The authors wish to thank Messrs. S. Nishihara and H. Kishida of Chuo Kaihatsu Corporation for their assistance in the preparation of this paper.

REFERENCES

1. Japan National Railway (1986). *Design Standard for Railway Retaining wall Structures* (in Japanese).
2. Murata, O., M. Tateyama and F. Tatsuoka (1994). "Shaking Table Tests on a Large Geosynthetic-reinforced Soil Retaining Wall Model", *Recent Case Histories of Permanent Geosynthetic-reinforced Soil Retaining Walls* (Tatsuoka and Leshchinsky eds.), A. A. Balkema, pp. 259-264.
3. Railway Technical Research Institute (1992). *Design Standard for Railway Earth Structures* (in Japanese).

4. Sato, T. (1996). "Estimation of Peak Ground Motion in the Severely Damaged Area during the 1995 Hyogoken-nambu Earthquake". *The 1995 Hyogoken-nambu Earthquake - An Investigation into the Damage to Civil Structures*. Committee of Earthquake Engineering, Japan Society of Civil Engineers, pp. 35-44.
5. Tatsuoka, F., M. Tateyama and J. Koseki (1996). "Performance of Soil Retaining walls for Railway Embankments", *A Special Issue of Soils and Foundations on Geotechnical Aspects of the January 17 1995 Hyogoken-nambu Earthquake*, pp. 311-324.